

THE CRYSTAL CHEMISTRY OF AEGIRINE FROM MONT SAINT-HILAIRE, QUEBEC

PAULA C. PIILONEN¹ AND ANDREW M. McDONALD²

Department of Earth Sciences, Laurentian University, Ramsey Lake Road, Sudbury, Ontario P3E 2C6

ANDRÉ E. LALONDE²

Ottawa – Carleton Geoscience Centre, Department of Earth Sciences, University of Ottawa, 140 Louis Pasteur Street, Ottawa, Ontario K1N 6N5

ABSTRACT

Aegirine from five different microenvironments within the peralkaline East Hill Suite (EHS) at Mont Saint-Hilaire, Quebec, were studied by SEM-EDS, Mössbauer spectroscopy, wet-chemical and ICP-MS methods. Pyroxene compositions range from aegirine-augite ($\text{Ae}_{38}\text{Di}_{39}\text{Hd}_{23}$) to end-member aegirine ($\text{Ae}_{97}\text{Di}_{1,5}\text{Hd}_{1,5}$); the crystals exhibit strong zoning, with a core enriched in Ca + Zr, and a rim enriched in Na + Ti. More than 85% of the Fe is present as octahedrally coordinated Fe^{3+} , suggesting conditions of extreme oxidation prior to aegirine crystallization. All samples of aegirine are enriched in the *REE* relative to chondrite and display a strong negative Eu anomaly. A concave pattern, with enrichments in both heavy and light *REE*, is found in all microenvironments except the one that led to fibrous aegirine. Such fibrous sprays show a steep, negative slope and are strongly enriched in the light *REE*. The aegirine is the product of fractionated batches of late-stage melt enriched in incompatible elements (*e.g.* Zr, Ti and *REE*) and Na. The extremely low $\text{Fe}^{2+}/\text{Fe}^{3+}$ values restrict pyroxene fractionation trends to the Di-Ae tie-line, unlike those noted elsewhere. The Ac and trace-element contents of the pyroxenes were used to develop an evolutionary scheme for the EHS. Fractional crystallization of a parental mafic magma, possibly accompanied by liquid immiscibility, resulted in the formation of nepheline and sodalite syenites. Further fractionation of the melt that gave sodalite syenite, enriched in volatiles and incompatible elements, led to crystallization of the aplites and pegmatite dikes, units which display identical aegirine, and to later igneous breccias. A secondary fluid-rich phase is considered responsible for very late-stage metasomatic overgrowths of fibrous aegirine in the pegmatite dikes.

Keywords: aegirine, peralkaline complex, clinopyroxene, chemical composition, Mössbauer spectroscopy, rare-earth elements, fractionation, Mont Saint-Hilaire, Quebec.

SOMMAIRE

Nous avons étudié l'aegyrine provenant de cinq microenvironnements dans la suite hyperalkaline de East Hill au mont Saint-Hilaire, Québec, par microscopie électronique à balayage avec dispersion d'énergie, spectroscopie de Mössbauer, analyse chimique par voie humide et par plasma à couplage inductif avec spectrométrie de masse. Les compositions de pyroxène vont d'augite aegyrinique ($\text{Ae}_{38}\text{Di}_{39}\text{Hd}_{23}$) au pôle aegyrine ($\text{Ae}_{97}\text{Di}_{1,5}\text{Hd}_{1,5}$); tous les cristaux font preuve de zonation marquée, à partir d'un noyau enrichi en Ca + Zr vers une bordure enrichie en Na + Ti. Plus de 85% du fer est à l'état ferrique et en coordination octaédrique, ce qui témoignerait d'une forte oxydation du magma avant sa cristallisation. Tous les échantillons d'aegyrine sont enrichis en terres rares par rapport aux chondrites, et montrent une forte anomalie négative en Eu. Un spectre concave des terres rares, c'est-à-dire avec des teneurs relativement élevées en terres rares légères et lourdes, caractérise l'aegyrine dans tous les milieux sauf celui qui a produit l'aegyrine fibreuse. De tels amas fibroradiés font preuve d'un spectre à forte pente négative, et donc avec un fort enrichissement en terres rares légères. L'aegyrine a cristallisé à partir de venues tardives de magma évolué, enrichi en éléments incompatibles (*e.g.*, Zr, Ti et les terres rares) et Na. A cause des valeurs extrêmement faibles du rapport $\text{Fe}^{2+}/\text{Fe}^{3+}$, les tracés d'évolution du clinopyroxène sont parallèles au vecteur Di-Ae, ce qui diffère des tracés d'autres complexes alcalins. La composition du clinopyroxène permet le développement d'un schéma évolutif pour la suite de East Hill. Une cristallisation fractionnée d'un magma parental mafique, possiblement accompagnée d'une immiscibilité du magma, a mené à la

¹ Present address: Ottawa – Carleton Geoscience Centre, Department of Earth Sciences, University of Ottawa, 140 Louis Pasteur Street, Ottawa, Ontario K1N 6N5. *E-mail address:* lattice@sympatico.ca

² *E-mail addresses:* amcdonal@nickel.laurentian.ca, aelsc@uottawa.ca

formation de syénites à néphéline et à sodalite. Un fractionnement plus poussé du magma qui a produit la syénite à sodalite, enrichi en composants volatils et en éléments incompatibles, a mené à la cristallisation d'aprites et de pegmatites en filons et à des brèches ignées tardives. L'aegyrine et l'assemblage de minéraux primaires sont identiques dans les aprites et pegmatites. Nous attribuons à une phase fluide secondaire la formation tardive métasomatique des amas fibroradiés en surcroissance dans les filons de pegmatite.

(Traduit par la Rédaction)

Mots-clés: aegyrine, complexe hyperalcalin, clinopyroxène, composition chimique, spectroscopie de Mössbauer, terres rares, fractionnement, mont Saint-Hilaire, Québec.

INTRODUCTION

Mont Saint-Hilaire (MSH), located 40 km east of Montreal, Quebec, is one of ten early Cretaceous alkaline intrusions collectively referred to as the Monteregian Hills (Adams 1903). The intrusions trend east-west along the junction of the St. Lawrence and Ottawa graben systems, from Mont Brome to the Oka carbonatite complex, rising abruptly from the surrounding St. Lawrence Lowlands. Mont Saint-Hilaire is composed of an older western and a younger eastern half, within which three main suites have been defined (Currie 1983, Currie *et al.* 1986): (1) the Sunrise suite consisting of amphibole-bearing alkaline gabbros, (2) the Pain de Sucre suite, composed of biotite gabbro and nepheline diorites, and (3) the East Hill Suite (EHS), composed of nepheline and sodalite syenites, pegmatite dikes, igneous breccias and associated rocks. The entire intrusion is mantled by a hornfels unit developed in the surrounding Ordovician host-rocks of the Lorraine and Richmond groups (Currie 1983, Currie *et al.* 1986). Radiometric dating of the intrusion has yielded an age of 125 Ma (Currie *et al.* 1986, Gilbert & Foland 1986, Fairbairn *et al.* 1963).

The Poudrette quarry within the EHS is a unique mineral locality from which 320 known mineral species, including more than 30 new to science, have been noted (Horváth & Gault 1990). The peralkaline nature of this intrusion accounts for the significant enrichment in incompatible elements such as the rare-earth elements (REE), Zr and Ti, which thus led to the crystallization of many of the exotic mineral species found there. Whereas a great deal of effort has been devoted to documenting the exotic mineralogy of MSH (*e.g.*, Chao & Wight 1995), little emphasis has been placed on the rock-forming minerals or the evolution the EHS. Owing to the extremely complex nature of the intrusion and the constant removal of material for road fill in the quarry workings, it has not been possible to map the EHS in detail to document the intrusive relationships among the numerous microenvironments. We have undertaken a crystal chemical study of aegyrine, a major rock-forming mineral within all microenvironments noted in the EHS, as a means of exploring the paragenesis and evolutionary history of this unique intrusion.

OCCURRENCE AND DESCRIPTION

The present study is based on samples of aegyrine collected from five different microenvironments exposed in the Poudrette quarry: miarolitic cavities in nepheline syenite, xenoliths of sodalite syenite, aprites, pegmatite dikes, and igneous breccias. Table 1 is a summary of the mineral assemblages in these microenvironments and a brief description of the aegyrine within each.

Dark grey, massive nepheline syenite (containing essential nepheline, plagioclase, kaersutite and annite) contains angular to rounded xenoliths of sodalite syenite up to a meter in width (Horváth & Gault 1990). The sodalite syenite xenoliths are host to a wide array of rare and unusual minerals, many of which have not been found in other microenvironments (Table 1). Aegyrine within these xenoliths occurs as dark brown to green, prismatic, subhedral to euhedral crystals that are typically 0.5 cm long, embedded in a matrix of sodalite. Optical studies using a Supper spindle stage and precession XRD reveal that such grains are actually intergrown polycrystalline aggregates oriented parallel to Z.

Spherical miarolitic cavities, ranging in diameter from one mm to 10 cm, occur within the massive, fine-grained nepheline syenite. These cavities are lined by euhedral analcime, aegyrine and natrolite, and are host to a wide array of REE and Ti silicates, oxides and carbonate minerals. Aegyrine from the miarolitic cavities occurs as small (0.5 cm) acicular crystals with a square cross-section and a characteristic blue-green color; they commonly are coated with epidote and an unknown Na-Ti silicate mineral.

Pegmatite dikes, which range from a few centimeters to a meter or more in width, cross-cut all other rock types within the EHS (Horváth & Gault 1990) and contain two generations of aegyrine. Coarse-grained, dark green to black aegyrine forms prismatic, subhedral to euhedral crystals ranging in length from one to 10 cm, with a square cross-section. These crystals are commonly oriented perpendicular to the dike margin, a reflection of inward growth into the dike. Larger crystals are commonly asymmetrical, exhibiting enhanced growth and thickening in the direction of magma flow within the dike. In contrast, a second generation of aegyrine occurs as light green, radiating, acicular sprays of terminated, euhedral crystals. These sprays are found on coarser grains of aegyrine and within small vugs.

TABLE 1. CHARACTERISTIC MINERAL ASSEMBLAGES OF THE MICROENVIRONMENTS WITHIN THE EAST HILL SUITE

Microenvironments	Mineralogy	Description of Aegirine
Miarolitic Cavities (MC)	analcime natrolite nepheline elpidite Ti-silicates and oxides	acicular, blue-green crystals (0.5 cm long) often coated by elpidite
Sodalite Syenite Xenoliths (SX)	sodalite natrolite villiaumite eudialyte astrophyllite biotite abundant REE minerals	dark green to brown, prismatic crystals 0.5 cm in length
Aplites (AP)	microcline albite natrolite	prismatic, dark green crystals 0.25-0.5 cm in length along with fibrous masses
Pegmatite Dikes (PEG)	natrolite catapleite microcline albite rhodochrosite analcime serandite astrophyllite zircon	coarse grained, subhedral to euhedral, prismatic crystals ranging in length from 1 to 8 cm with abundant fibrous, felted overgrowths
Igneous Breccias (IB)	quartz calcite molybdenite amphibole	dark green to brown crystals with red-brown terminations

A microenvironment previously undescribed from the EHS is here referred to as aplite. This unit is very fine grained, with a sugary texture. It is mineralogically equivalent to the pegmatite dikes, consisting of albite, microcline, natrolite and aegirine, and presumably represents the aplitic portion of zoned pegmatite dikes. However, field evidence required to substantiate this hypothesis is lacking. Aegirine within the aplite occurs as both fibrous, felted, acicular masses and as dark green, prismatic crystals ranging from 0.25 to 0.5 cm in length.

The igneous breccias contain fragments of material from all three suites at MSH. They display complex cross-cutting relationships with the previously described microenvironments exposed in the quarry. According to Currie (1983), the breccia locally contains fragments of younger syenite and phonolite, but elsewhere, pegmatite dikes, along with gabbroic dikes, are found to cross-cut breccia units. Such fragments are generally angular, range from a few centimeters to a meter in diameter, and may exhibit signs of partial melting and a reaction rim (Horváth & Gault 1990). Cavities within the breccias are

host to a unique suite of minerals. Aegirine occurs as prismatic, subhedral to euhedral, dark green to brown crystals with reddish brown terminations.

ANALYTICAL METHODS

Energy-dispersion spectrometry (SEM-EDS) and inductively coupled plasma - mass spectrometry (ICP-MS)

Major-element data were obtained using a JEOL 6400 SEM equipped with a Link Analytical energy-dispersion (ED) detector. All analyses were performed under the following operating conditions: accelerating voltage 20 kV, beam current 2.5 nA, and counting times of 100 seconds. Data reduction was performed using Link Analytical software and a ZAF4 correction. Additional analyses for F were conducted on a Cameca SX-50 electron microprobe, but concentrations above detection limits were not observed.

Six representative crystals were selected from each of the 22 specimens that were studied. These crystals were then mounted perpendicular to Z to evaluate the extent of

chemical zoning. A traverse was done on one crystal from each specimen; in addition, two core and two rim analyses were performed on each of the remaining five grains. The structural formulae were calculated on the basis of six atoms of oxygen, with the proportion of Fe^{2+} and Fe^{3+} estimated from charge-balance considerations and later determined by Mössbauer spectroscopy and wet-chemical methods.

Average concentrations of trace elements in aegirine concentrates were determined by ICP-MS. Crushed separates of approximately 0.1 g were digested in acid, and solutions were analyzed for the REE. Analyses of three samples (PEG17F, IB15, MC18) could not be done owing to the paucity of material available.

Determination of the ratio $\text{Fe}^{2+}/\text{Fe}^{3+}$

Mössbauer spectroscopy was employed to determine the proportion of Fe^{2+} and Fe^{3+} in selected specimens and to explore the possibility of Fe^{3+} in tetrahedral coordination. Two concentrates, PEG2 and SX10, representative of the pegmatites and the xenoliths of sodalite syenite, respectively, were chosen for analysis. Absorbers for the two specimens were prepared by crushing the separates in acetone to minimize oxidation of iron. For both absorbers, the ideal mass of material was calculated using the technique developed by Rancourt *et al.* (1993) to ensure the maximum signal-to-noise ratio. The powdered aegirine was suspended in petroleum jelly to ensure a random orientation of crystals within the circular aluminum mount (aperture: 1.0 cm, thickness: 0.6 cm).

Spectra were obtained using a ^{57}Co source in a rhodium matrix at room temperature (21°C). The transducer was employed in constant-acceleration mode over a Doppler velocity range of ± 4.0 mm/s, with the distance between absorber and source fixed at 12.5 mm. Spectra were calibrated with an ^{57}Fe -enriched iron foil. Data were collected in 1024 channels and folded to obtain a flat background. Spectra were fitted with the Voigt-based quadrupole splitting distribution method of Rancourt & Ping (1991).

In addition to the Mössbauer measurements, Fe^{2+} contents of the same samples were investigated by wet-chemical methods. Determinations were done by the Pratt method, with titrations performed on a Metrohm 670 titroprocessor using KMnO_4 . Standards included MRB-29 (in-house standard of basalt with an average value of 5.98 wt.% FeO) and FER-3 (CCRMP standard; Govindaraju 1994). Both standards and the two samples were digested in a 1:1:1 mixture of sulfuric acid, hydrofluoric acid, and water.

RESULTS

Back-scattered electron images (BSEI) reveal complex compositional zoning about Z in all samples. In most cases, this zoning is concentric, showing two or more chemically distinct zones separated by a sharp boundary (Fig. 1A). In addition, highly irregular, undulatory zoning also was observed, and possibly is due to the interaction of late-stage fluids with the grains (Fig. 1B). Inclusions of catapleiite are common within cores of the pitted or corroded grains that display this zoning

(Fig. 1C). Table 2 represents average results of the SEM-EDS analyses and chemical formulae for each sample.

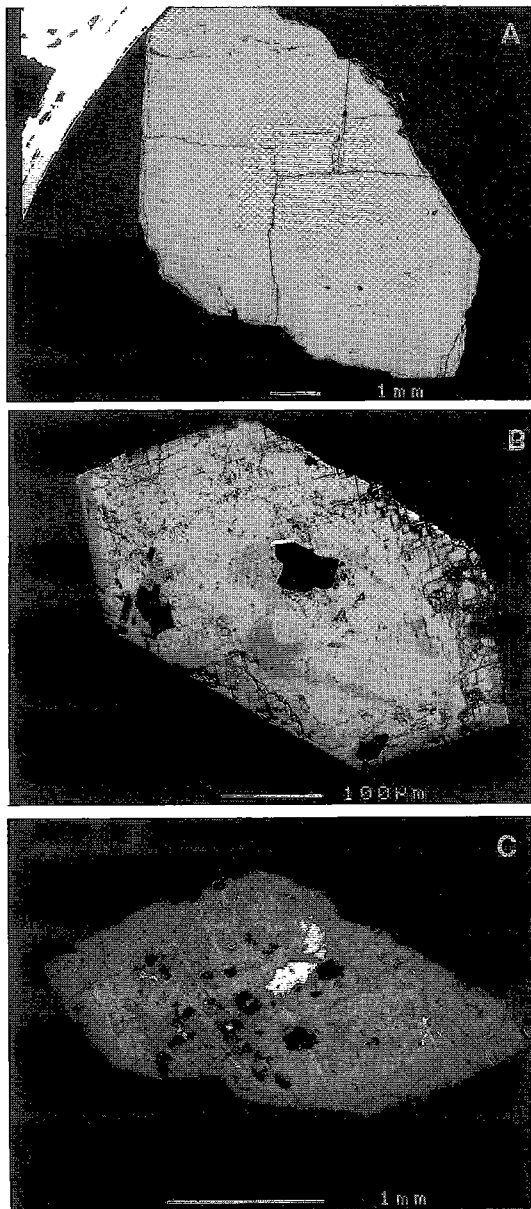


FIG. 1. Back-scattered electron images of aegirine from Mont Saint-Hilaire. A. Symmetrical, concentric zonation commonly observed in MSH aegirine, with a core (light grey) being enriched in Ca + Zr, and a rim (dark grey) enriched in Na + Ti. Scale bar: 1 mm. B. Irregular, undulatory zonation observed in many crystals, possibly due to late-stage interaction with metasomatic fluids. Scale bar: 100 μm . C. Catapleiite inclusion in aegirine core, indicating crystallization of secondary alkali zirconosilicate. Scale bar: 1 mm.

TABLE 2. AVERAGE COMPOSITIONS FOR AEGRINE FROM THE EAST HILL SUITE AT MONT SAINT-HILAIRE

Sample #*	PEG1C 31	PEG1F 4	PEG2C 34	PEG2F 4	PEG3C 28	PEG3F 4	PEG4 31	PEG5 36	PEG6 31	AP7 32	SX8 31
<i>Component oxides (wt.%)</i>											
SiO ₂	52.61	52.71	52.41	51.22	51.39	51.19	51.17	51.86	51.29	51.55	50.53
TiO ₂	0.67	1.29	0.59	0.96	0.72	1.17	0.88	1.63	1.89	0.74	1.54
ZrO ₂	1.44	1.00	1.07	0.43	1.20	0.73	1.28	0.83	0.94	0.39	0.34
Al ₂ O ₃	1.09	1.16	1.04	2.16	1.07	1.31	1.12	1.43	1.20	1.11	0.36
Fe ₂ O ₃	30.79	29.85	30.95	28.85	30.41	30.15	30.34	29.69	28.88	30.57	25.55
MnO	0.94	1.13	0.93	0.71	0.96	0.76	0.89	0.97	1.17	0.75	0.84
MgO	0.29	0.20	0.33	0.14	0.26	0.21	0.19	0.20	0.31	0.47	2.89
CaO	2.41	0.79	3.03	0.44	2.89	0.77	1.37	0.88	1.60	2.93	7.47
Na ₂ O	12.22	13.32	11.87	12.98	11.71	12.71	12.51	12.98	12.28	11.79	8.72
Total	102.46	101.45	102.22	97.88	100.61	98.99	99.74	100.47	99.55	100.29	98.24
<i>Number of cations on the basis of six oxygens</i>											
Si	1.98	1.99	1.97	1.99	1.96	1.98	1.97	1.97	1.97	1.97	1.96
Al ^{IV}	0.02	0.01	0.03	0.02	0.04	0.02	0.03	0.03	0.03	0.03	0.02
Sum	2.00	2.00	2.00	2.01	2.00	2.00	2.00	2.00	2.00	2.00	1.98
Na	0.89	0.97	0.85	0.98	0.85	0.95	0.93	0.94	0.92	0.88	0.61
Ca	0.10	0.03	0.13	0.02	0.14	0.03	0.05	0.05	0.07	0.12	0.37
Sum	0.98	1.01	0.98	1.00	0.98	0.98	0.99	0.99	0.98	0.99	0.97
Fe ³⁺	0.87	0.85	0.87	0.84	0.87	0.87	0.88	0.86	0.83	0.88	0.72
Fe ²⁺	0.00	0.00	0.01	0.01	0.01	0.00	0.01	0.00	0.00	0.00	0.00
Al ^{VI}	0.02	0.04	0.02	0.08	0.01	0.04	0.02	0.02	0.02	0.02	0.00
Ti	0.02	0.04	0.02	0.03	0.02	0.03	0.02	0.04	0.05	0.02	0.04
Zr	0.02	0.02	0.02	0.01	0.02	0.01	0.02	0.02	0.02	0.01	0.00
Mn	0.03	0.04	0.03	0.02	0.03	0.03	0.04	0.04	0.04	0.02	0.03
Mg	0.02	0.01	0.02	0.01	0.02	0.01	0.01	0.01	0.02	0.03	0.19
Sum	0.98	0.99	0.98	0.99	0.98	1.00	1.00	0.99	0.99	0.98	0.99
%Ae	89.36	96.07	85.66	97.44	85.41	96.01	93.44	94.17	92.00	87.21	59.05
%Di	5.72	2.26	7.44	1.35	7.51	2.31	3.36	3.20	4.47	7.01	24.57
%Hd	4.91	1.68	6.90	1.21	7.08	1.68	3.20	2.63	3.54	5.78	16.39

Sample #*	SX9 34	SX10 29	SX11 34	IB12 18	IB14 26	IB15 30	AP16 30	PEG17C 39	PEG17F 6	MC18 27
<i>Component oxides (wt.%)</i>										
SiO ₂	51.54	50.91	50.86	50.86	50.60	52.69	49.64	51.71	51.19	51.42
TiO ₂	0.53	0.45	1.97	1.25	1.73	0.85	1.11	0.80	1.17	2.19
ZrO ₂	0.52	0.42	0.48	0.56	0.39	0.07	0.79	1.17	0.73	0.33
Al ₂ O ₃	1.17	1.14	0.90	1.01	0.48	0.22	1.22	1.00	1.31	0.90
Fe ₂ O ₃	31.08	30.14	29.05	29.80	27.10	18.08	31.24	30.76	30.15	27.65
MnO	0.58	0.90	1.17	0.91	0.63	0.59	1.05	0.92	0.76	1.26
MgO	0.29	0.46	0.47	0.45	2.45	7.93	0.30	0.24	0.21	1.25
CaO	1.97	4.48	1.70	2.52	4.93	14.48	1.20	2.32	0.77	4.47
Na ₂ O	12.15	10.59	12.25	11.99	10.37	5.78	12.36	11.86	12.71	10.82
Total	99.83	99.48	98.85	99.34	98.67	100.69	98.91	100.77	98.99	93.13
<i>Number of cations on the basis of six oxygens</i>										
Si	1.98	1.96	1.97	1.96	1.96	1.97	1.97	1.97	1.98	1.96
Al ^{IV}	0.02	0.02	0.03	0.04	0.01	0.01	0.03	0.03	0.02	0.03
Sum	2.00	1.98	2.00	2.00	1.97	1.98	2.00	2.00	2.00	1.99
Na	0.89	0.77	0.93	0.87	0.75	0.43	0.95	0.86	0.91	0.79
Ca	0.09	0.21	0.07	0.13	0.25	0.56	0.05	0.11	0.07	0.19
Sum	0.98	0.98	1.00	1.00	0.99	1.00	1.00	0.97	0.98	0.98
Fe ³⁺	0.89	0.86	0.84	0.87	0.75	0.51	0.88	0.88	0.85	0.79
Fe ²⁺	0.01	0.00	0.00	0.01	0.00	0.00	0.00	0.00	0.01	0.00
Al ^{VI}	0.03	0.03	0.01	0.01	0.00	0.00	0.03	0.01	0.03	0.00
Ti	0.02	0.01	0.05	0.03	0.05	0.02	0.03	0.02	0.04	0.07
Zr	0.01	0.01	0.01	0.01	0.01	0.00	0.01	0.02	0.01	0.01
Mn	0.02	0.03	0.04	0.03	0.02	0.02	0.02	0.03	0.03	0.04
Mg	0.02	0.03	0.03	0.02	0.17	0.44	0.01	0.01	0.03	0.07
Sum	0.99	0.98	0.99	0.99	1.01	0.99	0.99	0.99	1.00	0.98
%Ae	90.15	78.44	91.27	86.03	69.31	37.52	93.78	88.02	90.76	77.43
%Di	5.25	11.38	5.06	7.31	19.23	39.89	3.45	6.23	5.28	12.97
%Hd	4.60	10.18	3.68	6.66	11.46	22.60	2.76	5.75	3.96	9.60

* # = number of analyses included in mean

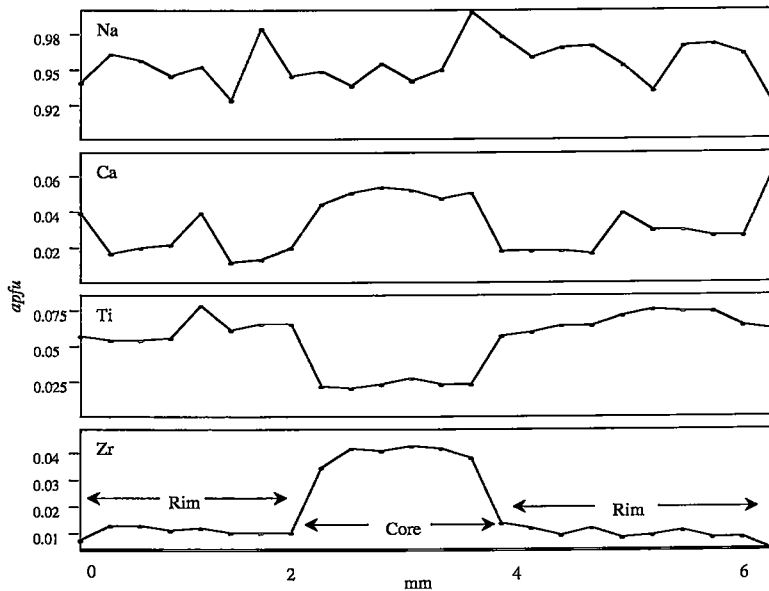


FIG. 2. Traverse across PEG5 from rim to rim, indicating the presence of a core enriched in Ca and Zr, and a rim enriched in Na and Ti. All traverses were performed perpendicular to Z.

Tetrahedral (T) site

Aegirine at Mont Saint-Hilaire displays almost complete occupancy of the *T* site by Si, with very limited substitutions. Silicon contents range from 1.96 to 1.99 atoms per formula unit (*apfu*), accompanied by minimal Al (range: 0.01–0.04 *apfu*), resulting in less than 2% Al ↔ Si substitution. The nearly complete occupancy of the *T* site by Si indicates that most of the remaining Al, along with Fe³⁺, Zr and Ti, must reside at the *M1* site. Previous investigators also have documented the presence of Al-poor clinopyroxene with negligible substitution of Al for Si in the *T* site in alkaline intrusions (e.g., Larsen 1976, Ramløv & Dymek 1991, Mitchell & Vladykin 1996).

M2 site

Sodium contents in the *M2* site range from 0.43 to 0.98 *apfu*. Aegirine from the pegmatites and aplites is the most enriched, whereas samples from the igneous breccias and sodalite syenite xenoliths display enrichments in Ca, resulting in up to 56% Na ↔ Ca substitution, and thus correspond to aegirine-augite. Traverses across individual grains (Fig. 2) reveal an antithetic relationship between Na⁺ and Ca²⁺, with cores rich in Ca and the rims enriched in Na (Fig. 3), a phenomenon consistent with increasing fractionation of the crystallizing magma (Deer *et al.* 1978). The strong 1:1 correlation ($R^2 = 0.99$) between Na and Ca noted in the aegirine points to a direct

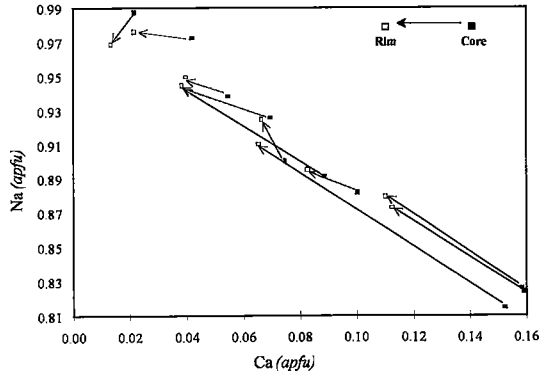


FIG. 3. Concentration of Ca versus that of Na, depicting core (closed squares) and rim (open squares) compositions in selected samples.

Na ↔ Ca substitution, resulting in a positive charge “excess” in the *M2* site of up to +0.56. The saturation of the *M2* site with Na, along with the deficiency in Al, are presumably due to the extreme peralkalinity of the parental magma, and are compensated by a net positive charge-deficiency within the *M1* site due to substitution of Mg, Fe²⁺ and Mn for Fe³⁺.

M1 site

The calculated Fe³⁺ content of the aegirine ranges from 0.51 to 0.89 *apfu*, with samples from the pegmatites displaying the highest contents. Charge-balance calculations indicate that all Fe present in the aegirine is Fe³⁺ (<0.01 *apfu* Fe²⁺). The pyroxene compositions display low Mg contents, relatively constant levels of Mn, and enrichments in both Ti (up to 3.38 wt.% TiO₂ in aegirine from the miarolitic cavity) and Zr (up to 3.27 wt.% ZrO₂ in aegirine from the pegmatites). Individual SEM-EDS traverses indicate that the core zone is enriched in Zr, whereas the rim is enriched in Ti, a trend similar to Ca and Na (Fig. 4). Variations in iron content from core to rim and the relationship of Fe to other cations can change dramatically, even within the same microenvironment.

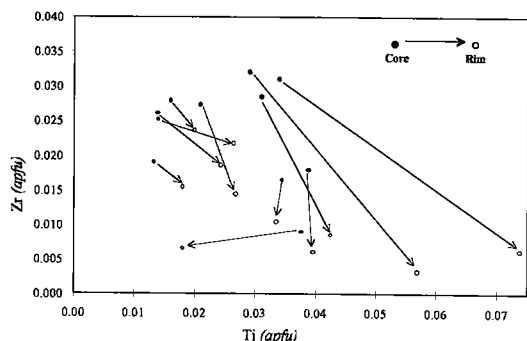


FIG. 4. Concentration of Ti versus that of Zr, depicting core (closed circles) and rim (open circles) compositions in selected samples.

The ratio Fe²⁺/Fe³⁺

The stoichiometric formulae calculated from the SEM-EDS analyses all suggest very low Fe²⁺ contents. This was confirmed by Mössbauer spectroscopy and wet-chemical determinations of FeO. It is important to note that the proportions of Fe²⁺ and Fe³⁺ obtained by these two methods apply to the bulk of each sample and do not take into consideration chemical zoning or inclusions that are present. Results and fitting parameters for each specimen can be found in Table 3.

TABLE 3. MÖSSBAUER SPECTRA FITTING PARAMETERS AND RESULTS FOR MSH AEGIRINE (PEG2 AND SX10)

Site	Site Component	Quadrupole Splitting (mm/s)	Centre Shift (mm/s)	# of Counts (h ⁺)	% Fe	
PEG2	Fe ³⁺	1	0.3032	0.3921	123114.2	88.4
		2	0.4937		45348	
		3	0.7163		23672.2	
Fe ²⁺	1	1.76	1.1519	10459.9	11.6	
	2	2.6861		13787.7		
Reduced $\chi^2 = 1.333$						
SX10	Fe ³⁺	1	0.3122	0.4054	103799.1	77.8
		2	0.4306		92463.8	
		3	0.7		39917.7	
Fe ²⁺	1	2.1766	1.1447	58047.1	22.2	
	2	2.7868		9436.2		
Reduced $\chi^2 = 0.778$						

The Mössbauer spectra are similar in the two specimens: both contain two prominent peaks positioned at approximately 0.3 and 0.6 mm/s that define the low- and high-energy lines, respectively, of the dominant Fe³⁺ doublet (Fig. 5). In addition, a less prominent and wide peak in the velocity range of 1.6 to 2.6 mm/s corresponds to the high-energy line of the Fe²⁺ doublet. The low-energy line of this doublet shows up as a shoulder on the low-energy Fe³⁺ line in the region of 0 mm/s.

The octahedrally coordinated Fe³⁺ was modeled as having three Gaussian contributions within a prominent doublet, with an average center shift at 0.39 mm/s (PEG2) and 0.41 mm/s (SX10). These values are nearly identical to that obtained by Annersten & Nyambok (1980) for pure, homogeneous aegirine from Arkansas (0.38 mm/s), but lower than that obtained by Singh & Bonardi (1972) for aegirine-augite from Joan Lake, Labrador (0.53 mm/s). The three contributions within the Fe³⁺ doublet are considered to represent variations in the local environment in which the cations reside.

The Fe²⁺ was modeled as having two distinct Gaussian contributions, which can easily be resolved as distinct peaks on the high-energy side of the spectrum, in the 1.5 to 2.5 mm/s range of velocity (Fig. 5). Center shifts for the samples are similar (PEG2: 1.15 mm/s; SX10: 1.14 mm/s), but lower than the values obtained by Annersten & Nyambok (1980), 1.6 mm/s, and Singh & Bonardi (1972), 1.30 mm/s. The Fe²⁺ doublets in SX10 are more prominent than those observed in PEG2, and indicate that 22.2% of the total iron is present as Fe²⁺, in contrast to 11.6% for PEG2. Average Fe²⁺ quadrupole splittings in the two spectra are nearly identical (PEG2: 2.29 mm/s, SX10: 2.26 mm/s).

Similar values for Fe²⁺/Fe_{tot} were obtained by wet-chemistry determinations. Table 4 presents a summary of results obtained by Mössbauer spectroscopy, Fe titrations, and SEM-EDS analyses. All indicate that greater than 85% of the total iron is present as octahedrally coordinated Fe³⁺ within the M1 site. Note that there is a discrepancy among results obtained by the three methods employed. The substantially lower Fe²⁺ contents suggested by the SEM-EDS data appear anomalous. Vacancies within the pyroxene structure, coupled with the initial calculation of total iron as Fe₂O₃, may have resulted in incorrect charge-balance, and thus low Fe²⁺/Fe³⁺ values.

TABLE 4. A COMPARISON OF RESULTS FROM MÖSSBAUER SPECTROSCOPY, SEM/EDS AND FeO TITRATIONS (WT. %)

Sample	Species	Mössbauer	SEM/EDS	FeO Titrations
PEG2	Fe ³⁺	27.36	30.75	28.78
	Fe ²⁺	3.59	0.32	2.17
SX10	Fe ³⁺	23.45	30.14	25.50
	Fe ²⁺	6.69	0.00	4.64

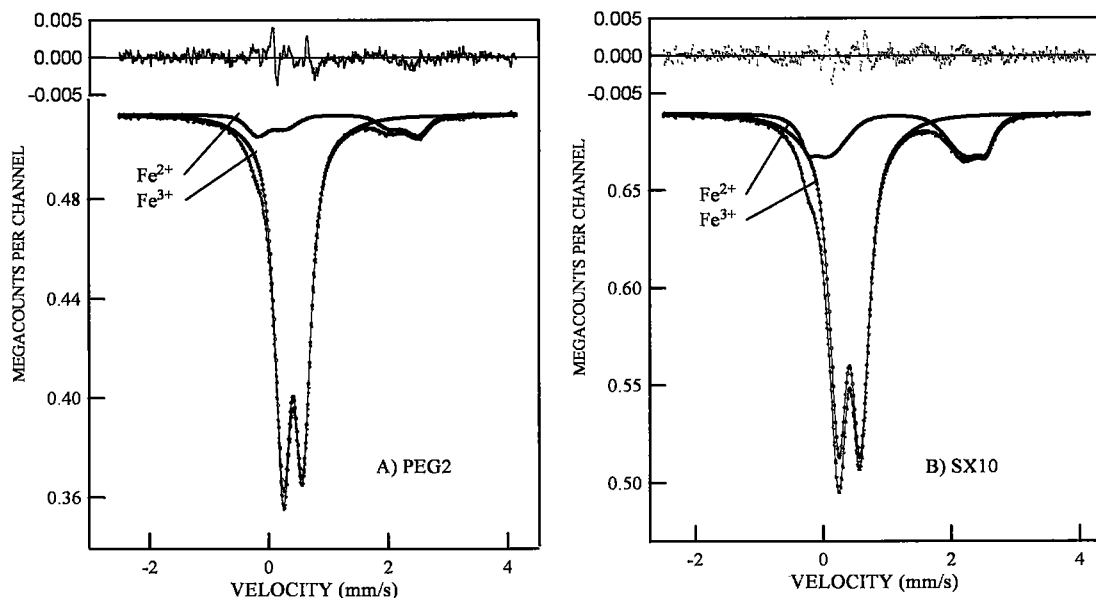


FIG. 5. Mössbauer spectra for aegirine from Mont Saint-Hilaire. A. PEG2: 88.4% Fe²⁺, 11.6% Fe³⁺. B. SX10: 77.8% Fe²⁺, 22.2% Fe³⁺. The solid line represents the best fit. Contributions corresponding to octahedrally coordinated Fe²⁺ and Fe³⁺ are superimposed on the data.

TABLE 5. RARE-EARTH ELEMENT CONCENTRATIONS (PPM) IN AEGIRINE FROM THE EAST HILL SUITE AT MONT SAINT-HILAIRE

Sample	La	Ce	Pr	Nd	Sm	Eu	Gd	Tb	Dy	Ho	Er	Tm	Yb	Lu
Sodalite syenite xenolith aegirine														
SX8	223.4	398.3	43.9	140.3	20.1	1.9	13.8	2.2	10.5	1.9	5.0	0.8	6.4	1.1
SX9	298.4	<i>n.d.</i>	82.7	281.7	42.3	3.8	29.2	4.3	20.5	3.6	8.5	1.2	7.1	1.1
SX10	41.7	103.7	12.9	44.3	7.5	0.6	4.8	0.8	4.1	0.8	2.9	0.8	8.9	2.1
SX11	44.8	88.3	9.4	30.5	5.0	0.4	3.5	0.6	3.0	0.7	1.8	0.4	4.2	0.9
Aplite aegirine														
AP7	26.1	42.2	4.7	16.7	2.9	0.3	1.8	0.3	1.8	0.4	1.9	0.6	6.8	1.6
AP16	199.4	418.0	46.9	151.5	23.1	2.2	17.3	2.8	13.1	2.2	5.0	0.7	5.2	1.0
Coarse pegmatite aegirine														
PEG1C	24.2	58.0	7.1	26.4	5.1	0.6	3.8	0.6	3.7	0.8	3.0	0.7	9.3	2.0
PEG2C	31.4	73.7	8.9	31.2	5.0	0.5	3.8	0.6	3.7	0.9	2.9	0.7	8.2	1.7
PEG3C	20.6	56.2	8.0	29.9	5.7	0.6	3.9	0.6	3.2	0.7	2.6	0.8	9.6	2.2
PEG4	17.5	42.3	5.6	20.7	3.9	0.4	2.5	0.4	1.9	0.4	1.6	0.5	6.2	1.4
PEG5	28.1	55.2	6.1	18.7	2.8	0.3	2.1	0.4	1.7	0.4	1.2	0.3	3.6	0.7
PEG6	27.3	60.2	6.9	23.0	4.2	0.4	2.9	0.5	2.2	0.4	1.3	0.3	3.5	0.7
PEG17	24.5	64.6	8.5	31.4	6.0	0.6	4.1	0.6	3.2	0.6	2.5	0.7	8.2	1.9
Fibrous pegmatite aegirine														
PEG1F	814.0	<i>n.d.</i>	112.1	354.4	61.5	5.9	42.6	6.6	32.4	6.1	17.9	3.0	19.3	2.7
PEG2F	224.3	464.4	56.3	183.4	44.0	5.4	45.3	8.8	49.8	9.0	21.2	2.9	15.2	1.9
PEG3F	303.0	1170	75.6	239.3	47.7	5.3	38.5	6.7	35.7	6.5	15.9	2.4	14.2	1.9
Igneous breccia aegirine														
IB14	67.7	152.9	17.8	62.6	11.3	1.4	9.1	1.5	8.8	1.8	5.7	1.2	11.5	2.2

n.d. - not detected

Rare-earth-element geochemistry

ICP-MS data indicate that the aegirine is enriched in the REE (Table 5), and display a strong, negative

europium anomaly that can be attributed to earlier fractionation of Ca-bearing minerals such as plagioclase and kaersutite, both of which occur in high modal percentages in the more primitive units of the EHS.

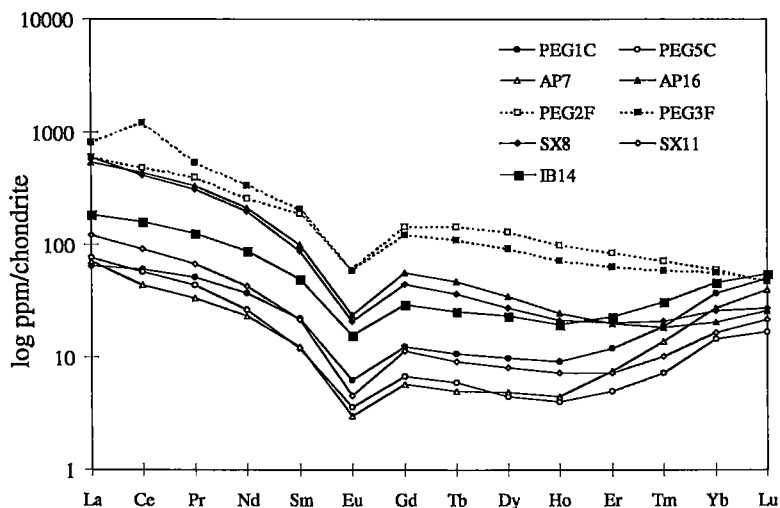


FIG. 6. Chondrite-normalized rare-earth-element abundances in aegirine from Mont Saint-Hilaire. The profiles for fibrous aegirine from pegmatite are shown as dashed lines.

Two distinct *REE* patterns were observed in the aegirine (Fig. 6). The first, observed in all specimens except the fibrous aegirine, is noticeably concave, with enrichments in both heavy *REE* and light *REE* relative to the middle *REE*, a pattern that seems inconsistent with *REE* patterns presented for other clinopyroxenes (Rollinson 1994). Of note are the *REE* patterns for the aegirine from aplite, which are identical to those of the aegirine from pegmatite, re-enforcing the hypothesis that both rock types are genetically related and possibly comagmatic.

The second *REE* pattern, observed only in the fibrous PEG aegirine, and to some extent in samples SX8 and AP16, exhibits greater enrichment in the light *REE* relative to both the middle and heavy *REE*, resulting in a negatively sloped trend with a strongly negative Eu anomaly. These samples display *REE* concentrations an order of magnitude greater than the previous ones.

DISCUSSION

Morimoto *et al.* (1989) defined aegirine as having more than 80% of the Ae end-member ($\text{NaFe}^3\text{Si}_2\text{O}_6$). Using this scheme of classification, the clinopyroxene analyzed in this study covers the range from aegirine-augite in the igneous breccias ($\text{Ae}_{38}\text{Di}_{39}\text{Hd}_{23}$) to near-end-member aegirine in the pegmatites ($\text{Ae}_{97}\text{Di}_{1.5}\text{Hd}_{1.5}$). At Mont Saint-Hilaire, the aegirine is unusual in that the Hd component never exceeds 23 mol.%, unlike that from most peralkaline intrusions (Fig. 7). In sodic peralkaline intrusions such as Itapirapua, Brazil (Gomes *et al.* 1970), South Qôroq, Greenland (Stephenson

1972), Ilfmaussaq, Greenland (Larsen 1976), and in alkaline ring complexes described by Bonin & Giret (1985), fractionation trends extend from Di further toward Hd (up to 95%) prior to crystallization of Ae (Fig. 7). In their study on clinopyroxenes from the Little Murun ultrapotassic complex (Aldan Shield, Russia), Mitchell & Vladykin (1996) found that the Hd contents did not exceed 15 mol.%, as at Mont Saint-Hilaire. In both cases, oxidation of iron had largely occurred prior to crystallization of the magma, thus inhibiting the crystallization of Fe^{2+} -bearing clinopyroxenes such as hedenbergite. Pyroxene trends observed by Mitchell (1980) in the Fen alkaline complex (Norway) and by Mitchell & Vladykin (1996) in the Little Murun Complex show more scatter than at Mont Saint-Hilaire, a feature that may be the result of competition for Ca–Mg–Na–Fe between the pyroxene and the other mafic phases. Within the EHS, aegirine is commonly the dominant mafic phase, resulting in a low degree of competition, thus producing a fractionation trend with minimal scatter. The fractionation trend established for the Mont Saint-Hilaire suite of pyroxene compositions appears to be unique among peralkaline intrusions.

The observed trend of continuous crystallization along the Di–Ae tie line indicates that the EHS is a product of fractionation of a volatile-rich, peralkaline magma enriched in Na and Fe^{3+} . The strong enrichments and distinct zonation of Zr and Ti within aegirine from MSH are directly related to this peralkalinity (Watson 1979, Farges *et al.* 1994). In most natural systems, Zr and Ti tend to behave independently and partition into Zr or Ti phases, or, if found in appreciable concentrations in a

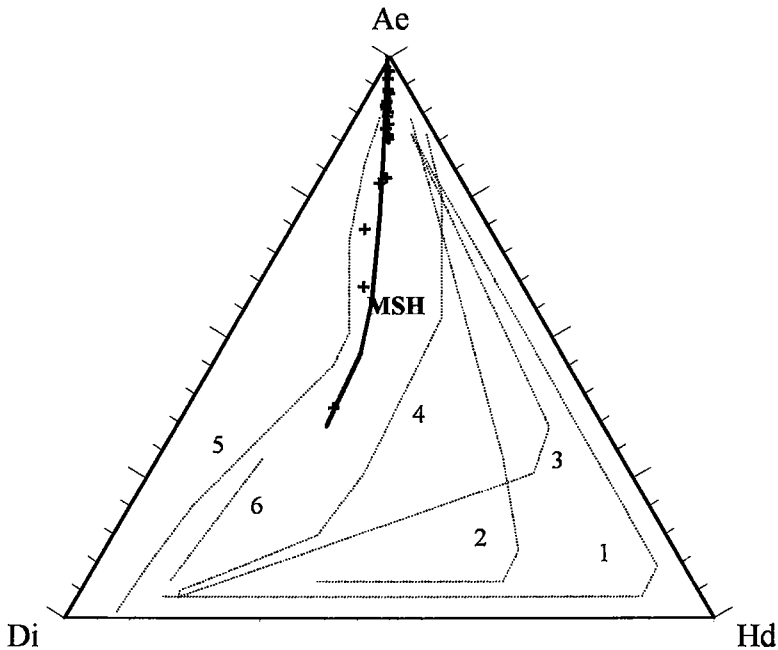


FIG. 7. Pyroxene crystallization trend at Mont Saint-Hilaire (solid line) compared to that obtained in similar alkaline intrusions (dashed lines). 1. Ilímaussaq, Greenland (Larsen 1976), 2. Morutu, Japan (Yagi 1966), 3. South Qôroq, Greenland (Stephenson 1972), 4. Auvergne, France (Varet 1969), 5. Little Murun ultrapotassic complex, Russia (Mitchell & Vladykin 1996), 6. Fen alkaline complex, Norway (Mitchell 1980).

single phase, will be strongly ordered (Pyatenko & Voronkov 1978). Such is the case at Mont Saint-Hilaire, where the core of the aegirine is enriched in Zr, and the rim in Ti. This so-called “peralkaline effect” (Farges *et al.* 1994) is the result of the chemical environment of the melt from which the pyroxene crystallized. Introduction of alkalis into a melt results in an increase of non-bridging oxygen atoms (*i.e.*, depolymerization of the melt), to which the Zr preferentially bonds. This depolymerization inhibits the formation of ^{71}Zr or ^{81}Zr and provides ideal sites for the formation of ^{61}Zr . Chain silicates crystallizing from this melt provide six-fold coordinated sites (*M1*) similar to those occupied by Zr in the melt, resulting in an increased crystal–melt partition coefficient and increased incorporation of Zr into the pyroxene structure.

This same mechanism may also be responsible for the incorporation of ^{61}Ti . However, unlike Ti, the coordination number of Zr is affected by the oxidation state of the melt in which it resides (Gomes *et al.* 1970, Watson 1979, Jones & Peckett 1980, Farges *et al.* 1994). Increased differentiation of the magma, coupled with decreasing $\text{Fe}^{2+}/\text{Fe}^{3+}$ values, favor the formation of charge-balanced $^{61}\text{Zr}-\text{O}-(\text{Si},\text{Na})$ bonds within the melt and an excess bond-valence in the *M1* site hosting the

Zr. As a result, zirconosilicates such as eudialyte or catapleite are more likely to crystallize, minerals in which the local environment around Zr is similar to that of Zr in the melt (Farges *et al.* 1994). Many minerals similar to these are observed in late-stage environments within the EHS at Mont Saint-Hilaire.

Although systematic variations in the ratio $\text{Fe}^{2+}/\text{Fe}^{3+}$ are not observed in the aegirine, the strong enrichment of Zr in the core and its depletion in the rim of crystals suggest that oxidizing conditions within the magma changed dramatically during crystallization of the pyroxene. Initial crystallization from a magma in which reduced conditions predominated resulted in aegirine enriched in the Di component and Zr. Continued enrichment in the Ae end-member resulted in Na and Fe^{3+} enrichment leading to decreased compatibility of Zr within the pyroxene structure, the formation of zirconosilicates, and Ae rims enriched in Ti.

Mont Saint-Hilaire is predominantly composed of mafic to intermediate gabbros, diorites and monzonites (Sunrise and Pain de Sucre suites), lithologic units that cannot be ignored when discussing the highly evolved syenites of the EHS. The EHS was emplaced through both older alkaline and country rocks, leading

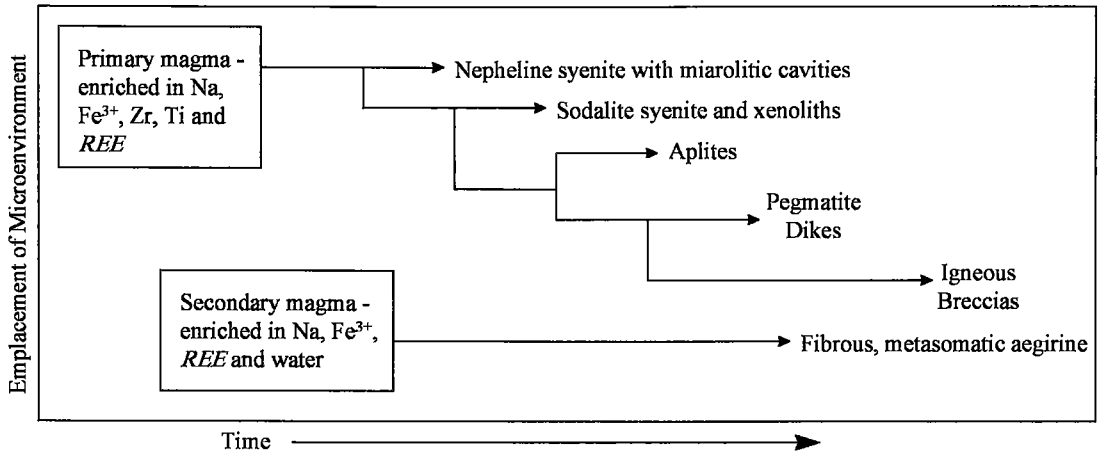


FIG. 8. Schematic representation of the paragenetic sequence for the evolution of the East Hill Suite at Mont Saint-Hilaire.

to assimilation and entrainment of xenoliths, following fractionation from a mafic parental magma (Currie 1983). The Ae content of the aegirine can be used to determine fractionation trends within the EHS. Increasing fractionation results in higher Ae contents, along with enrichments in trace elements such as Zr, Ti and REE (Deer *et al.* 1978). These systematic variations can be used to develop an evolutionary scheme for the EHS (Fig. 8).

The nepheline syenites and xenoliths of sodalite syenite are considered to be the most primitive, and thus the earliest-formed microenvironments within the EHS, as they display the lowest mol.% Ae and concentrations of incompatible trace elements. Field evidence demonstrates the presence of xenoliths of sodalite syenite in nepheline syenite and *vice versa*, with boundaries between host syenite and xenolith ranging from diffuse or smooth to irregular and angular. As such, these two microenvironments are considered to have formed contemporaneously from a single magma that may have undergone immiscibility at depth into two chemically distinct phases: (1) nepheline syenite, being less alkaline and more siliceous than (2) sodalite syenite, enriched in fluids and incompatible elements. The sodalite syenite may represent an exsolved, volatile-rich phase of the magma. The local mineralogy supports this hypothesis, as the sodalite syenite xenoliths are dominated by incompatible- and volatile-enriched minerals such as sodalite, natrolite, eudialyte and villiaumite, along with a variety of REE silicates and carbonates. Similarly, early crystallization of amphibole in the nepheline syenites indicates higher concentrations of SiO₂ and suggests a lower alkalinity, as alkali amphiboles such as kaersutite and arfvedsonite become increasingly unstable with increasing alkalinity in the magma (Stephenson 1972). Alkalinity appears to increase within the sodalite syenite xenoliths, as Ae contents and Zr concentrations

are generally elevated. Elevated Ti contents observed in aegirine from the miarolitic cavities suggest enrichment in a residual, fluid-rich melt during cooling of the nepheline syenite and formation of late-stage pockets. Increased Ti contents may also be the result of contamination from earlier mafic phases in the surrounding Pain de Sucre suite, which has been shown in previous studies to contain Ti-rich amphiboles and micas (Greenwood & Edgar 1984, Lalonde *et al.* 1996).

Following emplacement of the nepheline and sodalite syenites, pegmatite dike units formed within the EHS. These microenvironments show strong enrichment in the Ae component, Zr, Ti and REE, indicating increased fractionation and alkalinity. The aplitic units are considered to represent the outermost portions or chilled margins of these dikes. The aegirine in the aplite is generally slightly depleted in Zr, Ti and REE relative to the aegirine in the pegmatites. The pegmatite – aplite dikes appear to be the product of fractionation of the magma from which the syenites crystallized, as continuous trends are seen in terms of the system Ae–Di–Hd. Rare-earth patterns also display the same convex pattern as seen in the syenites, yet show stronger enrichments. It appears that this magma was fractionated from the fluid- and REE-rich batch from which the sodalite syenite xenoliths formed.

The fibrous aegirine found in the pegmatite dikes differs in both major- and trace-element concentrations from the associated coarse aegirine. These fibrous sprays are strongly enriched in the Ae component and depleted in both Zr and Ti. Although this may simply be a function of increasing peralkalinity and extreme removal of these two elements in earlier phases, the REE data suggest otherwise. Along with a strong enrichment in the REE, the fibrous aegirine displays a chondrite-normalized pattern with a steep, negative slope, distinct from the concave trend observed in the other specimens. The sprays of fibrous, skeletal aegirine may originate from a distinct,

later-stage, metasomatic event. The homogeneity of these samples (*i.e.*, lack of chemical or optical zonation) is consistent with this hypothesis. This metasomatic fluid may or may not have been directly related to previously crystallized microenvironments by normal processes of fractionation. The differences in major- and trace-element composition suggest that a second magma may have been involved.

In the past, there has been confusion surrounding the temporal relationship between the igneous breccias and the remainder of the microenvironments within the East Hill suite. The breccias are concentrated along the boundaries between the older Pain de Sucre and younger EHS, and contain clasts from both (Currie 1983, Horváth & Gault 1990). Complex cross-cutting relationships noted by Currie (1983) indicate pegmatite units cut by breccias, with the reverse also present, yet other authors fail to speculate on the relationships entirely. The igneous breccias are strongly enriched in Ti and depleted in Zr, and the clinopyroxene has a low Ae content, with a REE pattern identical to those for the syenites and pegmatites. They are considered to represent a very late-stage feature, emplaced contemporaneously with the pegmatite dikes. During fractionation within the earlier microenvironments, a trend toward Ti-enrichment can be seen, as aegirine rims contain elevated concentrations of Ti. Fractionation of the magma from which the pegmatites crystallized, coupled with contamination from Ti- and Ca-rich mafic rocks of the Pain de Sucre suite, may have resulted in a Ti-rich aqueous fluid that was emplaced explosively into zones of structural weakness between the two suites. It is unknown whether the igneous breccias were emplaced prior to or following the metasomatic event that produced the fibrous aegirine within the pegmatite dikes.

SUMMARY

1. At Mont Saint-Hilaire, clinopyroxene compositions range from to aegirine-augite ($Ae_{38}Di_{39}Hd_{23}$) to end-member aegirine ($Ae_{97}Di_{1.5}Hd_{1.5}$). All samples exhibit complex chemical and optical zonations. Cores are generally enriched in Ca + Zr, whereas rims are enriched in Na + Ti.

2. Mössbauer, Fe titrations and structural formulae all indicate that more than 85% of the total Fe is present as Fe^{3+} , and is presumably restricted to the M1 site.

3. The aegirine in this suite is enriched in REE relative to chondrite and shows a strong, negative Eu anomaly. However, two distinct patterns were noted. A concave pattern, with enrichments in both heavy and light REE, was observed in all microenvironments except the fibrous aegirine. REE patterns for these fibrous sprays are steep, with a negative slope, and are strongly enriched in the light REE.

4. Fractionation trends lie along the Di–Ae tieline as a result of low Fe^{2+}/Fe^{3+} values, unlike those observed in

geochemically similar intrusions. Aegirine at Mont Saint-Hilaire is the product of fractionated, late-stage, volatile-rich melts enriched in Na, Fe^{3+} , and incompatible elements such as Zr, Ti and the REE.

5. An evolutionary scheme was developed using fractionation trends and major- and trace-element distributions. The presence of nepheline and sodalite syenite is tentatively attributed to liquid immiscibility of a parental mafic magma following crystallization of the earlier Sunrise and Pain de Sucre suites. Pegmatite dikes and associated aplites were later emplaced within the EHS. Late-stage metasomatic activity resulted in the formation of fibrous, end-member aegirine within the pegmatites. The igneous breccia unit, contaminated by mafic rocks of the Pain de Sucre suite, was emplaced contemporaneously within the pegmatites along zones of structural weakness between the Pain de Sucre and East Hill suites.

ACKNOWLEDGEMENTS

The authors thank F. Ford, D. Crabtree and S. Miller of the MNDM Geoscience Laboratories for their assistance with the SEM–EDS and electron-microprobe analyses, along with providing use of the Rigaku diffractometer. Special thanks are extended to Dr. D.G. Rancourt of the Department of Physics, University of Ottawa, for use of the Mössbauer spectrometer and for all his input. Thanks are also extended to Dr. C.E.G. Farrow and Mr. N. Rowlands of INCO Exploration for use of the SEM and the polishing of sections. The comments and suggestions provided by two referees, Dr. K.L. Currie and Mr. R.A. Gault, along with additional comments by Drs. R.F. Martin, C.E.G. Farrow and T.S. Ercit, are greatly appreciated, and have increased the quality of this manuscript. We thank Mr. J.G. Poudrette for allowing access to the quarry site. This work was supported through grants from the Natural Sciences and Engineering Research Council and Laurentian University.

REFERENCES

- ADAMS, F.D. (1903): The Monteregian Hills – a Canadian petrological province. *J. Geol.* **11**, 239-282.
- ANNERSTEN, H. & NYAMBOK, I.O. (1980): The Mössbauer effect study of iron distribution in clinopyroxenes. *Kenya J. Sci. Tech.* **1**, 117-124.
- BONIN, B. & GIRET, A. (1985): Clinopyroxene compositional trends in oversaturated and undersaturated alkaline ring complexes. *J. Afr. Earth Sci.* **3**, 175-182.
- CHAO, G.Y. & WIGHT, Q. (1995): Mont Saint-Hilaire revisited. *2. Rocks and Minerals* **70**, 90-138.

- CURRIE, K.L. (1983): An interim report on the geology and petrology of the Mont Saint Hilaire pluton, Quebec. *Geol. Sur. Can., Pap.* **83-1B**, 39-46.
- _____, EBY, G.N. & GITTINS, J. (1986): The petrology of the Mont Saint-Hilaire complex, southern Québec: an alkaline gabbro – peralkaline syenite association. *Lithos.* **19**, 65-81.
- DEER, W.A., HOWIE, R.A. & ZUSSMAN, J. (1978): *Rock-Forming Minerals. 2A. Single-Chain Silicates*. Longman, Hong Kong.
- FAIRBAIRN, H.W., FAURE, G., PINSON, W.H., HURLEY, P.M. & POWELL, J.L. (1963): Initial ratio of strontium 87 to strontium 86, whole rock age and discordant biotite in the Monteregian igneous province, Québec. *J. Geophys. Res.* **68**, 6515-6522.
- FARGES, F., BROWN, G.E. & VELDE, D. (1994): Structural environment of Zr in two inosilicates from Cameroon: mineralogical and geochemical implications. *Am. Mineral.* **79**, 838-847.
- GILBERT, L.A. & FOLAND, K.A. (1986): The Mont Saint Hilaire plutonic complex: occurrence of excess ⁴⁰Ar and short intrusion history. *Can. J. Earth Sci.* **23**, 948-958.
- GOMES, C.D.B., MORO, S.L. & DUTRA, C.V. (1970): Pyroxenes from the alkaline rocks of Itapirapuã, São Paulo, Brazil. *Am. Mineral.* **55**, 224-230.
- GOVINDARAJU, K. (1994): 1994 compilation of working values and sample descriptions for 383 geostandards. *Geostandards Newsletter* **18**, 1-158.
- GREENWOOD, R.C. & EDGAR, A.D. (1984): Petrogenesis of the gabbros from Mt. St. Hilaire, Québec, Canada. *Geol. J.* **19**, 353-376.
- HORVÁTH, L. & GAULT, R.A. (1990): The mineralogy of Mont Saint-Hilaire, Quebec. *Mineral. Rec.* **21**, 284-359.
- JONES, A.P. & PECKETT, A. (1980): Zirconium-bearing aegirines from Motzfeld, South Greenland. *Contrib. Mineral. Petrol.* **75**, 251-255.
- LALONDE, A.E., RANCOURT, D.G. & CHAO, G.Y. (1996): Fe-bearing trioctahedral micas from Mont Saint-Hilaire, Québec, Canada. *Mineral. Mag.* **60**, 447-460.
- LARSEN, L.M. (1976): Clinopyroxenes and coexisting mafic minerals from the alkaline Ilfmaussaq intrusion, south Greenland. *J. Petrol.* **17**, 258-290.
- MITCHELL, R.H. (1980): Pyroxenes of the Fen alkaline complex, Norway. *Am. Mineral.* **65**, 45-54.
- _____, & VLADYKIN, N.V. (1996): Compositional variation of pyroxene and mica from the Little Murun ultrapotassic complex, Aldan Shield, Russia. *Mineral. Mag.* **60**, 907-925.
- MORIMOTO, N., chairman (1989): Nomenclature of pyroxenes. *Can. Mineral.* **27**, 143-156.
- PYATENKO, Y.A. & VORONKOV, A.A. (1978): Comparative crystal-chemical functions of titanium and zirconium in mineral structures. *Int. Geol. Rev.* **20**, 1050-1058.
- RANCOURT, D.G., McDONALD, A.M., LALONDE, A.E. & PING, J.Y. (1993): Mössbauer absorber thickness for accurate site populations in Fe-bearing minerals. *Am. Mineral.* **78**, 1-7.
- _____, & PING, J.Y. (1991): Voigt-based methods for arbitrary-shape static hyperfine parameter distributions in Mössbauer spectroscopy. *Nucl. Instrum. Methods Phys. Res.* **B58**, 85-97.
- RANLØV, J. & DYMEK, R.F. (1991): Compositional zoning in hydrothermal aegirines from fenites in the Proterozoic Gardar Province, South Greenland. *Eur. J. Mineral.* **3**, 837-853.
- ROLLINSON, H.R. (1994): *Using Geochemical Data: Evaluation, presentation, interpretation*. Longman Scientific & Technical, New York.
- SINGH, S.K. & BONARDI, M. (1972): Mössbauer resonance of arfvedsonite and aegirine-augite from the Joan Lake apgaitic complex, Labrador. *Lithos* **5**, 217-225.
- STEPHENSON, D. (1972): Alkali clinopyroxenes from the nepheline syenites of the South Qôroq centre, south Greenland. *Lithos*, **5**, 187-201.
- VARET, J. (1969): Les pyroxènes des phonolites du Cantal (Auvergne, France). *Neues Jahrb. Mineral., Monatsh.*, 174-185.
- WATSON, B.E. (1979): Zircon saturation in felsic liquids: experimental results and applications to trace element geochemistry. *Contrib. Mineral. Petrol.* **70**, 407-419.
- YAGI, K. (1966): The system acmite–diopside and its bearing on the stability relations on natural pyroxenes of the acmite – hedenbergite – diopside series. *Am. Mineral.* **51**, 976-1000.

Received September 11, 1997, revised manuscript accepted February 24, 1998.